

# Supplemental Materials:

## Methane retrieval from MethaneAIR using the CO<sub>2</sub> Proxy Approach: A demonstration for the upcoming MethaneSAT mission

August 28, 2023

### S1 Tuning of the A Priori Covariance Scaling Factor

Here we tune the regularization of the MethaneAIR retrieval by scaling the a priori covariance matrix via a parameter  $\gamma$ . In terms of the cost function  $J(\mathbf{x})$ ;

$$J(\mathbf{x}) = (\mathbf{y} - \mathbf{F}(\mathbf{x}))^T \mathbf{S}_o^{-1} (\mathbf{y} - \mathbf{F}(\mathbf{x})) + \gamma^{-2} (\mathbf{x} - \mathbf{x}_a)^T \mathbf{S}_a^{-1} (\mathbf{x} - \mathbf{x}_a) \quad (\text{S1})$$

For the observations to be useful for estimating methane emissions, to first order the appropriate choice of  $\gamma$  is guided by the need to generate a 1:1 response to boundary layer CH<sub>4</sub> concentrations. The vertical sensitivity of the retrieval is quantitatively expressed through the column averaging kernel  $\mathbf{a}_{\text{CH}_4}$ , which represents the fractional change in retrieved methane vertical column  $\hat{N}_{\text{CH}_4}$  relative to a perfect observing system where departures from the prior are perfectly fitted. Following Connor et al. (2008) the column averaging kernel element for the  $l^{\text{th}}$  layer is related to the CH<sub>4</sub> profile component of the state vector  $\mathbf{x}_{\text{CH}_4}$  by

$$a_{\text{CH}_4, l} = \frac{1}{h_l} \frac{\partial \hat{N}_{\text{CH}_4}}{\partial x_{\text{CH}_4, l}} = \frac{1}{h_l} \mathbf{h}^T \mathbf{A}_{\text{CH}_4} \quad (\text{S2})$$

Here  $\mathbf{A}_{\text{CH}_4}$  corresponds to the block of the retrievals averaging kernel covered by the profile scale factors.  $\mathbf{h}$  is the column operator that maps the retrieved scale factors to the methane column (i.e.  $N_{\text{CH}_4} = \mathbf{h}^T \mathbf{x}_{\text{CH}_4}$ ). Similar expressions exist for the CO<sub>2</sub> averaging kernel. The a priori covariance matrices for CH<sub>4</sub> and CO<sub>2</sub> largely control the averaging kernel responses. Here we use those from the UoL GOSAT retrieval algorithm (Figure S1). Early testing on  $15 \times 3$  (across  $\times$  along track) pixel aggregates suggested that CH<sub>4</sub> was under-regularized relative to CO<sub>2</sub> (not shown here), likely due to the lower spectral information content for MethaneAIR relative to GOSAT. As a result the original CH<sub>4</sub> matrix was reduced by a factor of 9 to produce unit boundary layer column averaging kernel values. After the scaling the uncertainty is still loose relative to that expected from nature, with standard deviations  $>300$  ppbv in the boundary layer (Figure S1).

In this paper retrievals were performed at native and  $5 \times 1$  pixel aggregations. To maintain a uniform surface response  $\gamma$  must be retuned due to the noise increase from the lower pixel aggregation. If  $\gamma_n$  corresponds to the tuned value for the  $n$ -pixel aggregate, it can easily be shown that the same averaging kernel for an  $m$  pixel aggregate should be

$$\gamma_m^2 = \frac{m}{n} \gamma_n^2 \quad (\text{S3})$$

To show this, the averaging kernel  $\mathbf{A}$  is related to the retrieval gain matrix  $\mathbf{G}$  by

$$\mathbf{G} = \left( \mathbf{K}^T \mathbf{S}_o^{-1} \mathbf{K} + \frac{1}{\gamma^2} \mathbf{S}_a^{-1} \right)^{-1} \mathbf{K}^T \mathbf{S}_o^{-1} \quad (\text{S4})$$

$$\mathbf{A} = \mathbf{G} \mathbf{K} \quad (\text{S5})$$

Where  $\mathbf{K}$  is the jacobian of the forward model. Let  $\mathbf{S}_{o, n}$  be the observation error covariance for an  $n$ -pixel aggregation. By the central limit theorem  $\mathbf{S}_{o, n} = \frac{m}{n} \mathbf{S}_{o, m}$ . Matching the averaging kernel requires matching the gain.

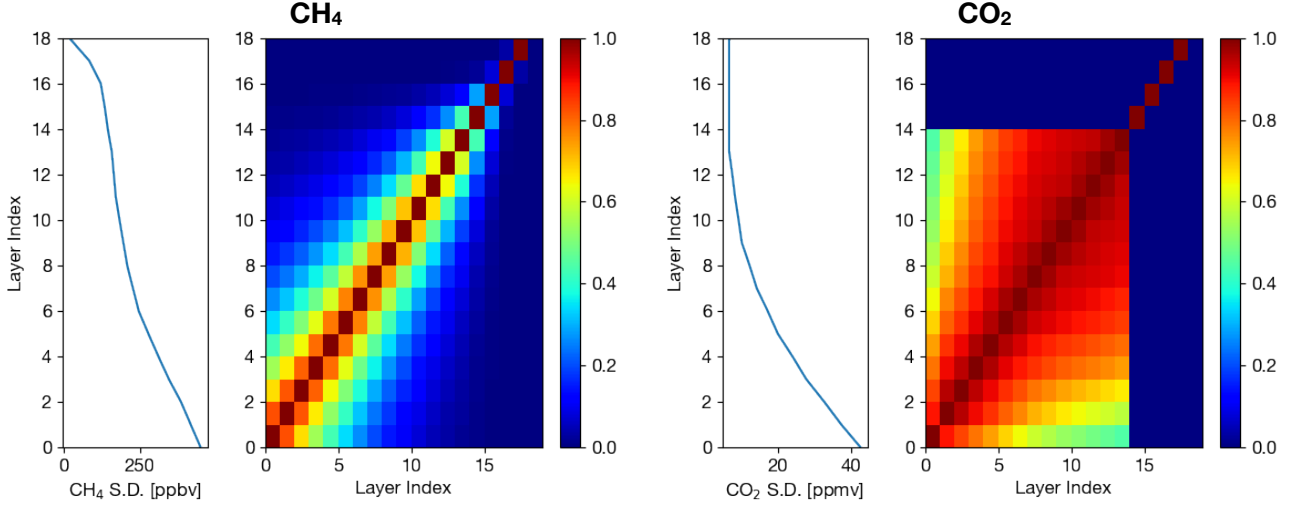


Figure S1: A priori error covariance matrices for  $\text{CH}_4$  and  $\text{CO}_2$  used by the MethaneAIR retrieval. The covariance matrices have been decomposed into layer standard deviation profiles (left) and correlation matrices (right).

$$\mathbf{G}_n = \left( \mathbf{K}^T \mathbf{S}_{\mathbf{o},n}^{-1} \mathbf{K} + \frac{1}{\gamma_n^2} \mathbf{S}_{\mathbf{a}}^{-1} \right)^{-1} \mathbf{K}^T \mathbf{S}_{\mathbf{o},n}^{-1} \quad (\text{S6})$$

$$= \frac{n}{m} \left( \frac{n}{m} \mathbf{K}^T \mathbf{S}_{\mathbf{o},m}^{-1} \mathbf{K} + \frac{1}{\gamma_n^2} \mathbf{S}_{\mathbf{a}}^{-1} \right)^{-1} \mathbf{K}^T \mathbf{S}_{\mathbf{o},n}^{-1} \quad (\text{S7})$$

substituting equation S3

$$\begin{aligned} \mathbf{G}_n &= \frac{n}{m} \left( \frac{n}{m} \left( \mathbf{K}^T \mathbf{S}_{\mathbf{o},m}^{-1} \mathbf{K} + \frac{1}{\gamma_m^2} \mathbf{S}_{\mathbf{a}}^{-1} \right) \right)^{-1} \mathbf{K}^T \mathbf{S}_{\mathbf{o},n}^{-1} \\ &= \left( \mathbf{K}^T \mathbf{S}_{\mathbf{o},m}^{-1} \mathbf{K} + \frac{1}{\gamma_m^2} \mathbf{S}_{\mathbf{a}}^{-1} \right)^{-1} \mathbf{K}^T \mathbf{S}_{\mathbf{o},m}^{-1} \\ &= \mathbf{G}_m \end{aligned} \quad (\text{S8})$$

To tune the regularization we perform a set of retrievals,  $\gamma^2$  is systematically varied over a range of  $10^{-4}$  to  $10^4$  using a  $5 \times 1$  aggregated MethaneAIR observation from the return leg of RF06. We select an observation with relatively low signal to ensure that signal-dependent artifacts caused by over-regularization are minimized. In this case the solar zenith angle was  $46^\circ$ , and albedo 0.17, making it within the lowest 5 percentile of albedos observed during the return leg. The resulting dependence of the  $\text{CO}_2$  and  $\text{CH}_4$  averaging kernels is shown in Figure S2 (middle, right). As  $\gamma^2$  increases, the column averaging kernels tend towards 1, with both species having 1:1 responses for  $\gamma^2 \geq 10$ . This confirms the original tuning performed on the  $15 \times 3$  pixel aggregates, as based on Equation S3 we would expect to loosen the regularization by a factor of 9. In all cases there remains a steep drop off in the averaging kernel sensitivity above 200 hPa. This corresponds to the airmass above the aircraft, and occurs because light is only traversing the layers above once.

Selecting values of  $\gamma$  larger than 10 marginally improves the vertical sensitivity, at the cost of worsening the measurement precision. The appropriate trade-off point can be determined heuristically using the L-curve method (Hansen, 1993), which compares the two components of  $J(\mathbf{x})$  (Equation S1) (i.e. the norm of the spectral residuals versus the norm of the difference between the retrieved and a priori state) at different  $\gamma$ . Figure S2 (left) shows the L-curve for the test pixel. At high regularization (low  $\gamma$ ) increasing  $\gamma$  reduces the spectral fit residuals without significant increases in the regularization norm, indicating over-regularization. At the other extreme (high  $\gamma$ ), increasing  $\gamma$  mostly increases the regularization norm, reflecting the situation where measurement noise starts dominating the retrieved state. The trade-off point where the retrieval does not under/overfit the spectrum can be estimated as the point of maximum curvature between these two extremes. From Figure S2 this occurs within  $\gamma^2 = 0.1 - 10$ . In consideration of this and the averaging kernel boundary layer response we select  $\gamma^2 = 10$  for the  $5 \times 1$  observation and scale to  $\gamma^2 = 50$  for the native resolution (Equation S3).

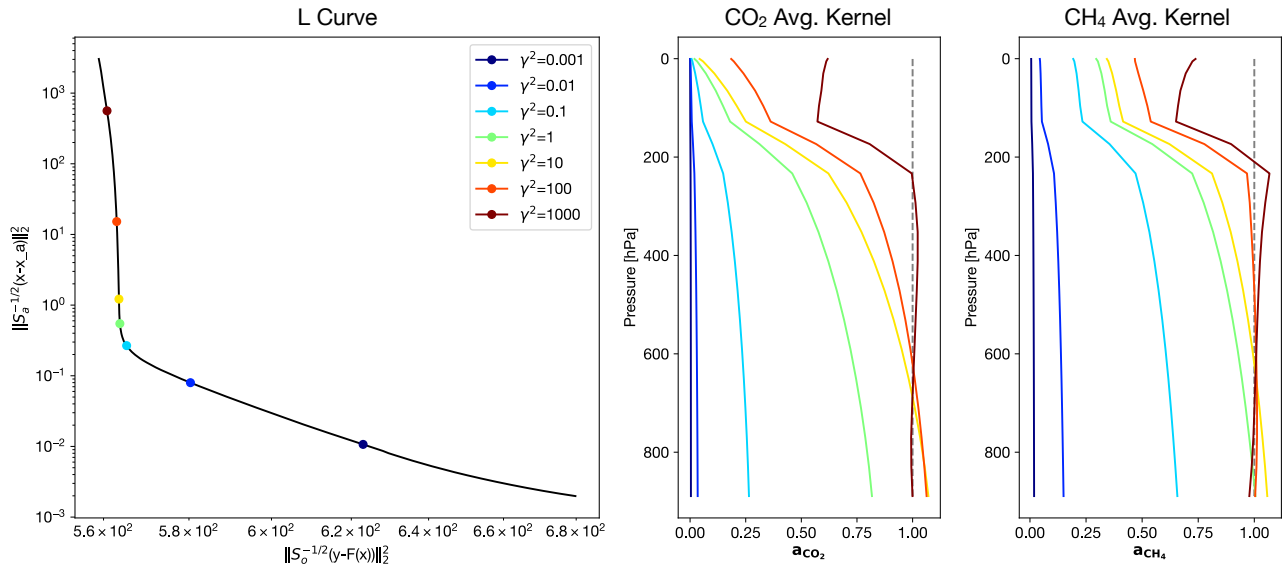


Figure S2: L-Curve and CO<sub>2</sub>/CH<sub>4</sub> column averaging kernels for the test pixel used to tune the MethaneAIR regularization factor for the  $5 \times 1$  pixel aggregation (see text).

Figure S3 shows the CO<sub>2</sub> and CH<sub>4</sub> degrees of freedom for signal (DoFS) for all pixels for the RF06 return leg as a function of albedo. The DoFS are the trace of the the averaging kernel CO<sub>2</sub>/CH<sub>4</sub> sub-matrices, and is a measure of the individual pieces of profile information that can be constrained by the retrieval. Figure S3 shows that there is a steep drop off in the DoFS curve for CO<sub>2</sub> starting at  $\sim 0.10$  albedo. Below this value the retrieved CO<sub>2</sub> column will increasingly be dominated by the prior. The drop-off in CH<sub>4</sub> DoFS occurs at smaller signal levels, indicating that the retrieval is limited by the CO<sub>2</sub> light path constraint. The majority of scenes corresponding to the prior-dominated signal levels correspond to those over water.

## References

Connor, B. J., Boesch, H., Toon, G., Sen, B., Miller, C., and Crisp, D.: Orbiting Carbon Observatory: Inverse method and prospective error analysis, *Journal of Geophysical Research: Atmospheres*, 113, <https://doi.org/10.1029/2006JD008336>, eprint: <https://onlinelibrary.wiley.com/doi/pdf/10.1029/2006JD008336>, 2008.

Hansen, P. C.: *The L-curve and its use in the numerical treatment of inverse problems*, 1993.

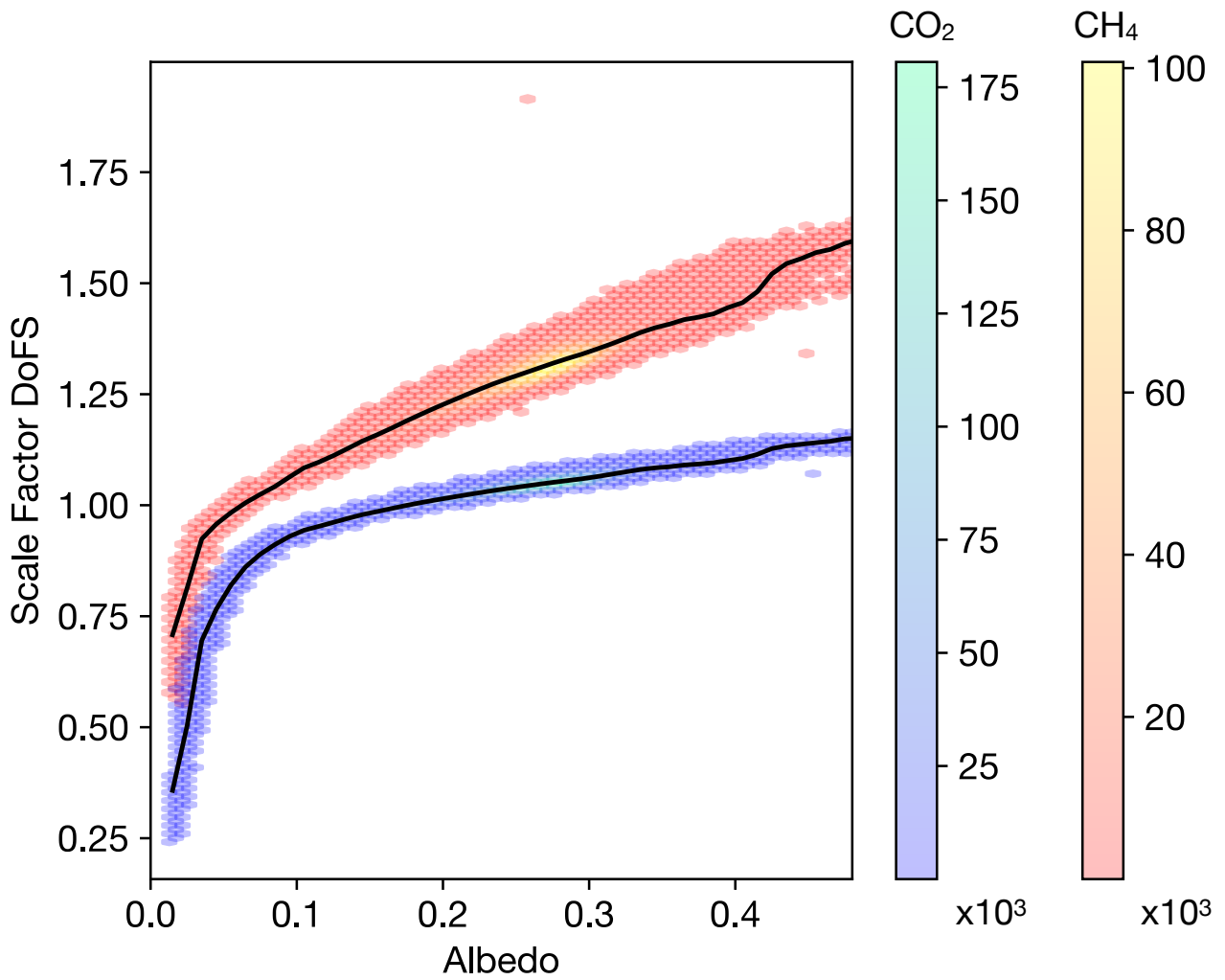


Figure S3: CO<sub>2</sub> and CH<sub>4</sub> degrees of freedom for signal as a function of scene albedo for the return segment used to determine albedo XCH<sub>4</sub> (see main text). Color maps represent observation density.